Miniature Q-Band GaAs Bandpass Filters in Heterodyne Receiver for Radio Astronomy

Y.-S. Lin, W.-H. Liao, and Y.-S. Hsieh
Department of Electrical Engineering, National Central University
Chungli 320, Taiwan, R.O.C.

***Abstract*- We report on the design and experimental results of Q-band bandpass filters for the Atacama Large Millimeter/ submillimeter Array (ALMA) band-1 receiver. The bandpass filter is required to reject the lower side band from 15.3 to 29 GHz while retain minimum insertion loss across the passband of 31.3 to 45 GHz. In order to largely reduce the size and weight of receiver module, on-chip bandpass filter designs in GaAs pHEMT process are proposed. The parallel-coupled bandpass filter with quarter-wavelength resonators is adopted to achieve a wide fractional bandwidth of about 37%. In addition, the capacitive/inductive loaded coupled-line and the stepped-impedance resonator are used to largely reduce the filter size. Moreover, the cross-coupling effect is introduced to create transmission zeros, such that the required stopband rejection below 29 GHz can be achieved. Specifically, two GaAs bandpass filters with sizes less than 0.9 mm×0.6 mm and 1.0 mm×0.8 mm are demonstrated, which are smaller than our previous published work. They will be applied to the multi-chip-module version of ALMA band-1 receiver prototype for further system evaluation and feasibility studies.**

I. INTRODUCTION

The Atacama Large Millimeter/submillimeter Array (ALMA) is a millimeter/sub-millimeter wave interferometer to be located at an altitude of about 5000 meters in Llano de Chajnantor, Chile. It covers the frequency range of 31 to 950 GHz, which is divided into 10 bands coinciding with those transparent atmospheric windows. The ALMA band-1 receiver, which set the RF frequency range from 31.3 to 45GHz, is believed to be capable of solving important scientific topics including high-resolution Sunyaev-Zel'dovich effect imaging, cosmic microwave background, high-redshifted extragalactic CO lines, and probing of magnetic field strength via Zeeman measurements [1].

Shown in Fig. 1 is the front-end block diagram of ALMA band-1 receiver, and the detail system specification can be found in [1]. The main purpose of the bandpass filter is to reject the lower side band from 15.3 to 29GHz by 25dB so as to ensure single sideband operation. The required performance on in-band (31.3 to 45GHz) insertion loss is within 1dB, with a return loss better than 15dB and a group delay variation within 0.25ns. Originally the bandpass filter is designed using the WR22 rectangular waveguide structure as shown in Fig. 2 [2]. Considering the requirement of dual-polarization, 2-stage cascade RF amplifier modules plus the mixer and waveguide bandpass filter, then the mechanical size and weight will be larger than the upper limit of the receiver cartridge. In addition, since the RF LNA and mixer at the input and output of the bandpass filter are all based on GaAs MMICs, two additional microstrip-to-waveguide transitions are required to connect them to the WR22 waveguide bandpass filter. This introduces additional loss by about 1dB, not including the possible mismatch loss at the junctions.

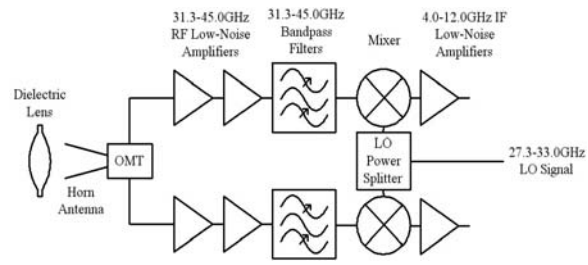

Figure 1. Block diagram of the ALMA band-1 heterodyne receiver front-end in this study.

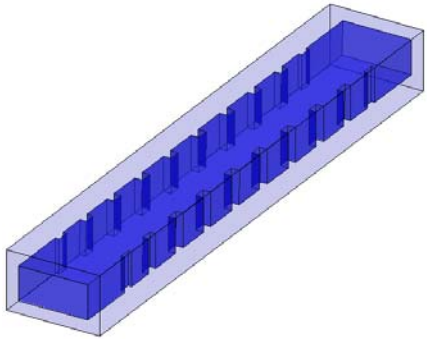

(a)

(b)

Figure 2. (a) 3D view and (b) photograph of the 9th-order WR22 waveguide bandpass filter based on inductive iris for ALMA band-1 from [1].

On the other hand, on-chip planar filter realization will reduce the complexity of module assembly effectively by implementing the receiver in the multi-chip module (MCM) design. Also, both the size and weight of receiver module can be largely reduced in this way at the expense of higher insertion loss compared to waveguide filter design. Some previous works on the design of on-chip millimeter-wave bandpass filter have been done in [3]-[5]. Although very compact circuit sizes can be achieved, the selectivity of them is not so good. In our previous work [6], two Q-band bandpass filters based on GaAs process are proposed to achieve very compact circuit size as well as excellent selectivity. They can meet the stringent requirements of ALMA band-1 receiver as well as reduce the receiver size and complexity of receiver module assembly effectively. In this work, further size reduction of these GaAs bandpass filters are proposed to facilitate the further integration with other MMIC's when implementing the receiver.

II. Filter Design

A. Filter Type-I

Shown in Fig. 3 are the chip photo and circuit model of proposed Type-I microstrip bandpass filter of 6th-order. This filter is an extension of the parallel-coupled bandpass filter with quarter-wavelength (λ/4) resonators [7]. Since the required bandwidth is around 37%, the input and output couplings are modified to tapped-input form so as to achieve larger amount of coupling. Like that in [6], the capacitive and inductive loaded coupled-line structures [8]-[11] can be adopted to reduce the filter size. In addition, the stepped-impedance λ/4 resonator is also used such that the length of the coupled-line can be reduced to as short as λ/16. As a result, very compact filter size can be achieved.

In order to meet the required rejection of 25dB below 29GHz, two transmission zeros are introduced by enhancing the magnetic cross-coupling M between the two microstrip short-stubs as indicated in Fig. 3(b). In this way, the filter topology becomes a 6th-order cascade quadruplet one, and the quasi-elliptic response can be obtained to enhance the selectivity.

Based on the requirements of ALMA band-1 receiver, the filter is designed according to similar procedures in [10]-[11] using the WIN 0.5μm E/D-mode pHEMT process on 4mil GaAs substrate [12]. The chip size is only 1.5×1.0mm^2, and the filter size is about 1.0×0.8mm^2 not including the input and output pads. The measured and EM simulated results are shown in Fig. 4. Good agreement between them is observed. The measured in-band insertion loss is less than 2.9dB from 31.3 to 45GHz, with a minimum insertion loss of 1.35dB at 38GHz. The in-band return loss is better than 16.9dB. Two transmission zeros at 28.5GHz and 48.4GHz are observed as expected, and the rejection of lower side band (15.3 ~ 29GHz) is better than 31dB.

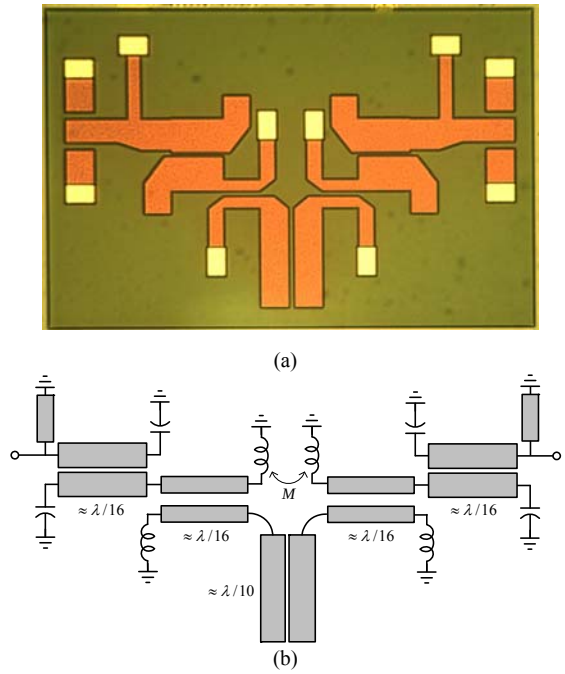

Figure 3. (a) Chip photograph and (b) circuit model of the Type-I Q-band GaAs bandpass filter for ALMA band-1. (Chip size: 1.5×1.0mm^2.)

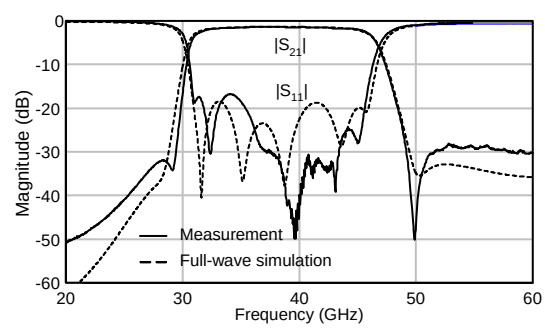

Figure 4. Measured and full-wave simulated results of the Type-I Q-band GaAs bandpass filter.

B. Filter Type-II

To further reduce the filter size and loss, the Type-II design shown in Fig. 5 is also implemented. Since the receiver specification only requires the rejection of lower side band, a cascade trisection filter that exhibits one transmission zero at the lower stopband can be adopted. In this way, the required rejection can be obtained with lower filter order, such that both the filter size and loss can be further reduced. The Type-II filter in Fig. 5 is also based on an extension to the 4th-order parallel-coupled bandpass filter with λ/4 resonators [7], with the input and output couplings modified to tapped-input form. Again, the inductive loaded coupled-line is used to reduce the circuit size. In addition, two cross-coupling capacitors C_c are introduced between resonator pairs (1, 3) and (2, 4) through microstrip gaps so as to achieve transmission zeros at the lower stopband.

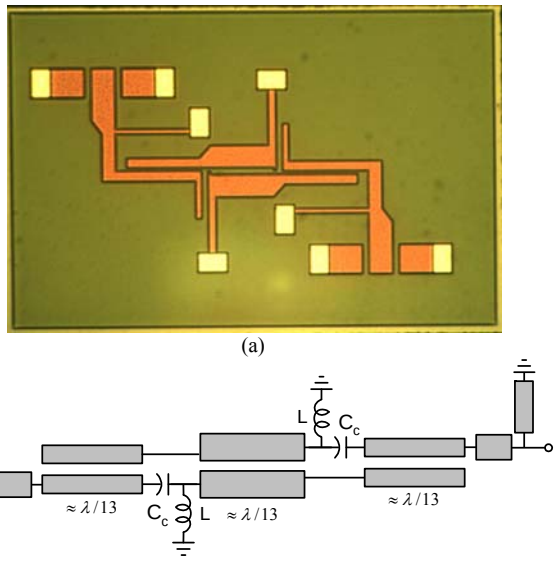

Figure 5. (a) Chip photograph and (b) circuit model of the Type-II Q-band GaAs bandpass filter for ALMA band-1. (Chip size: 1.5×1.0mm^2.)

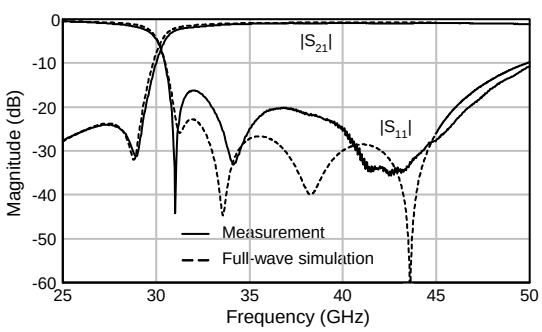

Figure 6. Measured and full-wave simulated results of the Type-II Q-band GaAs bandpass filter.

The Type-II filter is implemented using the same GaAs pHEMT process. Shown in Fig. 6 are the measured and EM simulated results. Good agreement between them is observed. The measured in-band insertion loss is less than 2.2dB from 31.3 to 45GHz, with a minimum insertion loss of 0.88dB at 38GHz. The in-band return loss is better than 16.2dB. One transmission zeros in the lower stopband is observed at 28.9GHz, which is due to the cross-coupling capacitors C_c. The rejection of lower side band is better than 24dB. The chip size is only 1.5×1.0mm^2, and the filter size is only about 0.9×0.6mm^2. Note that both the insertion loss and filter size are improved compared to the Type-I filter.

The sizes of the proposed Type-I and Type-II GaAs bandpass filters are only around $0.37\lambda_g \times 0.30\lambda_g$ and $0.33\lambda_g \times 0.22\lambda_g$ at the center frequency, respectively. They are smaller than the filters in [6]. In addition, they are much smaller and lighter-weight when compared with the original WR22 waveguide design, which has an outer dimension of 30mm×30mm×40mm. Fig. 7 compares the measured insertion loss responses of the two proposed GaAs bandpass filters with the 9th-order WR22 waveguide bandpass filter in Fig. 2. Their in-band insertion losses are all within 3dB. The rejections at 29GHz for these three filters are about the same. Although the insertion loss is larger by about 0.5~2.3dB compared to the WR22 waveguide filter, with the proposed GaAs bandpass filters, one may save two waveguide-to-microstrip transitions and the additional insertion and mismatch losses associated with them. The module assembly can also be greatly simplified. In addition, since the bandpass filter is at the LNA output, the higher insertion loss of the GaAs bandpass filter should have minimum impact on the receiver noise temperature, and can be easily compensated by manipulating the gain budgets of the LNA and mixer.

Fig. 8 shows the measured in-band group delay responses of the proposed GaAs filters and the WR22 waveguide filter. Since the proposed GaAs filters employ lower filter order to achieve compact circuit size and additional transmission zeros to improve filter selectivity, their group delays are lower than that of the WR22 waveguide one. Also, the in-band group delay variations are all within the specified 0.25ns for the two GaAs bandpass filters, which are slightly better than that of the WR22 waveguide one.

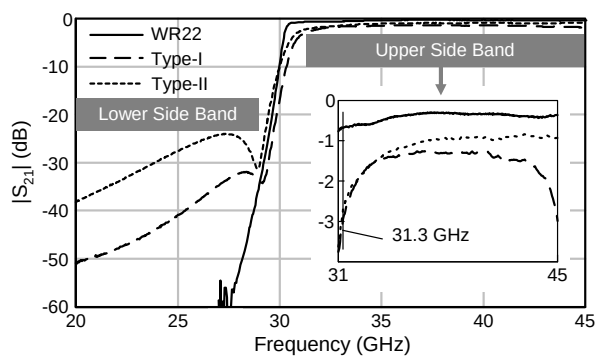

Figure 7. Measured transmission coefficients of the two proposed GaAs bandpass filters and the 9th-order WR22 waveguide bandpass filter shown in Fig. 2.

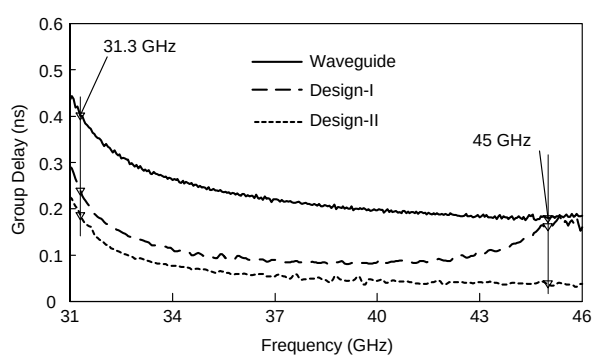

Figure 7. Measured group delays of the two proposed GaAs bandpass filters and the 9th-order WR22 waveguide bandpass filter shown in Fig. 2.

III. Conclusion

In this paper, Q-band bandpass filters for ALMA band-1 receiver are presented. To largely reduce the module size, weight, and complexity of module assembly, two compact planar bandpass filters in GaAs process are demonstrated. They can achieve very good selectivity and lower sideband rejection, and can be easily integrated in the receiver. They will be applied to the MCM version of the heterodyne receiver prototype design for ALMA band-1.

Acknowledgment

This work was supported in part by the National Science Coucil, Taiwan, R.O.C. under Grants NSC97-2221-E-008-034-, NSC95-2745-M-001-001, and NSC 96-2911-M-001-005-MY3, and by the National Center for High-Performance Computing, Taiwan, R.O.C. The authors would like to thank the WIN Semiconductor Corporation, Taiwan, R.O.C. for the support of GaAs pHEMT process.

References

[1] Y.-J. Hwang, C.-C. Chiong, S.-W. Chang, T. Wei, W.-T. Wong, Y.-S. Lin, M.-T. Chen, H. Wang, and H.-Y. Chang, "Cryogenic testing and multi-chip module design of a 31.3~45GHz MHEMT MMIC-based heterodyne receiver for radio astronomy," in *Proc. SPIE Astronomical Instrumentation Conf.*, vol. 7020, 70201v, 2008.

[2] Y.-S. Lin, Y.-S. Hsieh, Y.-J. Hwang, C.-C. Chiong, "Q-band bandpass filter designs in heterodyne receiver for radio astronomy," in *2008 IEEE Asia-Pacific Conference on Circuits and Systems*, pp. 86-89, Dec. 2008.

[3] E. van der Hejden, M. Notten, G. Dolmans, H. Veenstra, and R. Pijper, "On-chip third-order band-pass filters for 24 and 77 GHz car radar," in *IEEE MTT-S Int. Microw. Symp.* Dig., pp. 697-700, Jun. 2006.

[4] M.-F. Lei and H. Wang, "Implementation of reduced-size dual-mode ring filters in LTCC and MMIC processes at millimeter wave frequencies," in *36th European Microwave Conf. Proc.*, pp.537-540, 2006.

[5] B. Dehlink, M. Engl, K. Aufinger, and H. Knapp, "Integrated bandpass filter at 77GHz in SiGe Technology," *IEEE Microwave Wireless Comp. Lett.*, vol. 17, no. 5, pp. 346-348, May 2007.

[6] Y.-S. Lin, Y.-S. Hsien, C.-C. Chiong, and Y.-J. Hwang, "Q-Band GaAs bandpass filter designs for ALMA band-1," *IEEE Microwave Wireless Comp. Lett.*, vol. 19, no. 6, pp. 353-355, June 2009.

[7] Y.-S. Lin, P.-Y. Chang, and Y.-S. Hsieh, "Compact electronically switchable parallel-coupled microstrip bandpass filter with wide stopband," *IEEE Microwave Wireless Comp. Lett.* vol. 18, no. 4, pp. 254-256, April 2008.

[8] Y.-S. Lin, H.-M. Yang, and C. H. Chen, "Miniature microstrip parallel-coupled bandpass filters based on lumped-distributed coupled-line sections," in *IEEE MTT-S Int. Microwave Symp. Dig.*, pp.691–694, June 2005.

[9] R. Phromloungsri, M. Chongcheawchamnan, and I. D. Robertson, "Inductively compensated parallel coupled microstrip lines and their applications," *IEEE Trans. Microw. Theory Tech.*, vol. 54, no. 9, pp. 3571–3582, Sep. 2006.

[10] Y.-S. Lin, and C.-C. Cheng, "Miniature CPW parallel-coupled bandpass filter based on inductive loaded coupled-lines and lumped-element J-inverters," *IEEE Microwave Wireless Comp. Lett.,* vol. 17, pp. 343-345, May. 2007.

[11] Y.-S. Lin, and C.-C. Cheng, "Miniature microstrip bandpass filters based on capacitive loaded coupled-lines and lumped-element K-inverters," *IEICE Trans. Electron.*, vol. E90-C, no. 12, pp. 2218-2225, Dec. 2007.

[12] WIN Semiconductor Corporation. http://www.winfoundry.com/..